Published in final edited form as:
Invest Ophthalmol Vis Sci. 2009 February ; 50(2): 870–877. doi:10.1167/iovs.08-2376.

Lipoprotein Particles of Intraocular Origin in Human Bruch Membrane: An Unusual Lipid Profile

Lan Wang[1], **Chuan-Ming Li**[1], **Martin Rudolf**[1,2], **Olga V. Belyaeva**[3], **Byung Hong Chung**[4], **Jeffrey D. Messinger**[1], **Natalia Y. Kedishvili**[3], and **Christine A. Curcio**[1]

1 *Department of Ophthalmology, University of Alabama at Birmingham, Birmingham, Alabama*

3 *Department of Biochemistry and Molecular Genetics, University of Alabama at Birmingham, Birmingham, Alabama*

4 *Department of Nutritional Biochemistry and Genomics, University of Alabama at Birmingham, Birmingham, Alabama*

Abstract

Purpose—Throughout adulthood, Bruch membrane (BrM) accumulates esterified cholesterol (EC) associated with abundant 60- to 80-nm-diameter lipoprotein-like particles (LLP), putative apolipoprotein B (apoB) lipoproteins secreted by the retinal pigment epithelium (RPE). In the present study, neutral lipid, phospholipids, and retinoid components of human BrM-LLP were assayed.

Methods—Particles isolated from paired choroids of human donors were subjected to comprehensive lipid profiling (preparative liquid chromatography [LC] gas chromatography [GC]), thin-layer chromatography (TLC), high-performance liquid chromatography (HPLC), Western blot analysis, and negative stain electron microscopy. Results were compared to plasma lipoproteins isolated from normolipemic volunteers and to conditioned medium from RPE-J cells supplemented with palmitate to induce particle synthesis and secretion.

Results—EC was the largest component (32.4 ± 7.9 mol%) of BrM-LLP lipids. EC was 11.3-fold more abundant than triglyceride (TG), unlike large apoB lipoproteins in plasma. Of the fatty acids (FA) esterified to cholesterol, linoleate (18:2n6) was the most abundant (41.7 ± 4.7 mol%). Retinyl ester (RE) was detectable at picomolar levels in BrM-LLP. Notably scarce in any BrM-LLP lipid class was the photoreceptor-abundant FA docosahexaenoate (DHA, 22:6n3). RPE-J cells synthesized apoB and numerous EC-rich spherical particles.

Conclusions—BrM-LLP composition resembles plasma LDL more than it does photoreceptors. An EC-rich core is possible for newly synthesized lipoproteins as well as those processed in plasma. Abundant EC could contribute to a transport barrier in aging and lesion formation in age-related maculopathy (ARM). Analysis of BrM-LLP composition has revealed new aspects of retinal cholesterol and retinoid homeostasis.

Age-related maculopathy (ARM) is the leading cause of new, untreatable vision loss in the elderly of industrialized nations. [1] Its main clinical and histopathologic lesions affect the retinal pigment epithelium (RPE; support cells for photoreceptors), Bruch membrane (BrM; a thin intima-like extracellular matrix), and the choriocapillaris vessels, ultimately impacting vision

Corresponding author: Christine A. Curcio, Department of Ophthalmology, 700 South 18th Street, Room H020, Callahan Eye Foundation Hospital, University of Alabama School of Medicine, Birmingham, AL 35294-0009; E-mail: curcio@uab.edu.
[2]Present affiliation: University Eye Hospital Lübeck, Universitäs-klinikum Schleswig-Holstein, Lübeck, Germany.

Disclosure: **L. Wang**, None; **C.-M. Li**, None; **M. Rudolf**, None; **O.V. Belyaeva**, None; **B.H. Chung**, None; **J.D. Messinger**, None; **N.Y. Kedishvili**, None; **C.A. Curcio**, None

by the photoreceptors.[2] Early ARM is characterized by drusen (focal extracellular debris), basal linear deposit (BlinD; a diffusely distributed drusenoid material), and altered RPE morphology and pigmentation. This disease stage has limited treatment options, including antioxidant nutritional supplements, and, in its later stages, loss of eyesight is possible. Although some gene sequence variants increase ARM risk,[3] the largest risk factor for early ARM remains advanced age. It is therefore important to understand how age-related changes in the affected tissues impel some individuals toward severe disease.

Lipoproteins are naturally occurring nanoparticles composed of lipid and protein held together by noncovalent forces. Each particle is a microemulsion consisting of a surface of phospholipids (PLs), unesterified cholesterol (UC), and apolipoproteins and a core of neutral lipids, principally esterified cholesterol (EC) and triglyceride (TG). Lipoprotein classes differ in relative amount of lipids, protein/lipid ratio, and apolipoprotein species present, resulting in differences in size, density, and electrophoretic mobility. Lipoprotein classes containing apoB are chylomicrons (CM; from intestine), very-low-density lipoproteins (VLDL; from liver), and LDL (metabolite of VLDL). ApoB lipoproteins must be properly lipidated by their source cells in order for particle maturation and secretion to proceed. Core lipid composition reflects the availability of input FA and the substrate preferences of catalytic enzymes in upstream pathways.[4]

From late adolescence through senescence, BrM in normal human eyes markedly accumulates histochemically detectable EC associated with abundant 60- to 80-nm-diameter solid lipoprotein– like particles (LLP).[5–8] Further, drusen contain EC, UC, and immunoreactivity for apos A-I, B, C-I, C-II, and E.[9] This deposition is not necessarily attributable to the systemic aging phenomenon by which EC from LDL accumulates in connective tissues, including arterial intima and cornea.[10] Rather, recent evidence implicates EC as part of an apoB lipoprotein constitutively produced within the eye by the RPE and secreted into BrM, where it participates in ARM progression. Native human RPE expresses apolipoprotein mRNA transcripts, the proteins of apos B-100 and E, and notably, microsomal triglyceride transfer protein (MTP), required for apoB secretion and the product of the abetalipoproteinemia gene.[11,12] Isolated BrM-LLP segregate into the appropriate band of a density gradient but differ from plasma lipoproteins in cholesterol profile.[13] Cultured RPE secretes apoE, primarily into a high-density fraction.[14]

Size and lipid composition are strongly related for apoB lipoproteins, in that particles >25 nm diameter (CM and VLDL) have TG-rich cores and smaller particles (including LDL) have EC-rich cores.[15] BrM-LLP, as large as VLDL or small CM, are expected to be TG-rich. Indeed, an early assay of BrM/choroid indicated 1.77-fold more moles TG than EC.[16] However, other studies in which polarizing microscopy in tissue sections[6] and enzymatic assay in isolated particles[13] were used indicate that EC predominates over TG by at least threefold. To facilitate insight into the biological function of BrM-LLP and improve understanding of the lipids available to form the characteristic ARM extracellular lesions, we used comprehensive profiling of neutral lipid, PL, and retinoid components of BrM-LLP isolated from human donor eyes, comparing these results to plasma apoB lipoproteins and the secreta of an RPE cell line.

Methods

Preparation of Human Donor Eyes and Isolation of Particles

Human tissue use conformed to the Declaration of Helsinki and institutional review at the University of Alabama, Birmingham (UAB). BrM-LLP were isolated from BrM/choroids (Fig. 1A) of 11 paired donor eyes (Table 1), as described.[13] From BrM/choroids of four donors, total lipids were extracted without prior lipoprotein isolation (Table 1). Changes consistent with ARM were noted in 4 of 15 donors. We processed donor eyes in the order received, and

we did not analyze the ARM eyes separately, because there were too few to permit valid conclusions. Peripheral drusen were present in all older eyes. Flattened choroids (Fig. 1A) were scanned for area determination (described later). Supernatants generated from three rounds of tissue homogenization, centrifugation, and resuspension in isolation buffer[13] containing 1 M NaCl[17] were pooled. The pellet (BrM remainder) was saved at −80°C for separate analysis. Density was adjusted to 1.24 g/mL (by weight) by adding solid KBr, overlaid with 1 mL of 1.21 g/mL KBr, and centrifuged (49,000 rpm, 36 hours, 10°C, SW41Ti rotor, L80 ultracentrifuge, Beckman, Fullerton, CA). One half milliliter of each supernatant ($d \leq 1.21$ g/mL, lipoprotein-containing, called the top fraction) and infranatant ($d > 1.21$ g/mL, lipoprotein-sparse, called the bottom fraction) were withdrawn (Fig. 1B) for various assays.

Preparation of Human Plasma Lipoproteins

Plasma from four normolipemic volunteers, obtained at ~4 postprandial hours, was pooled to maximize the CM sample. Lipoproteins were isolated as described.[13]

One-Dimensional Thin Layer Chromatography (TLC)

Lipids were extracted from BrM-LLP, BrM remainders, medium, and cells by using chloroform-methanol (2:1 vol/vol).[18] Aliquots of organic phase were evaporated under nitrogen, resolubilized in chloroform, and applied to TLC plates (LHPKD silica gel 60A, Whatman, Florham Park, NJ) as described.[12] For separation of EC, TG, UC, FA, PE, and PC, plates were developed in petroleum ether:diethyl ether:acetic acid (84:15:1). For greater separation of PL and sphingomyelin (SPM), plates were developed in chloroform: methanol: ammonium hydroxide (65: 25:4). Plates were sprayed with 3% copper acetate in 8% phosphoric acid solution and heated to reveal bands. Standards were chloroform-solubilized 1,2-dioleoyl-sn-glycero-3-phosphocholine, oleate, triolein, cholesteryl oleate, SPM (esterified to mostly palmitate, 16:0), and UC (SPM from Avanti Polar Lipids, Alabaster AL; others from Sigma-Aldrich, St. Louis, MO). For semiquantitative assessment, plates were scanned, bands were defined within contrast-inverted images, and band intensities were measured (IPLab; BioVision Technologies, Exton, PA).

Comprehensive Lipid Profiling

BrM-LLP, plasma lipoproteins, and BrM/choroids were characterized by Lipomics (West Sacramento, CA) using preparative liquid chromatography (LC), gas chromatography (GC), and flame ionization detection. Lipids were extracted[18] in the presence of authentic internal standards. Individual lipid classes within each extract were separated by LC (model 1100 series; Agilent Technologies, Palo Alto, CA). Each lipid class was transesterified in 1% sulfuric acid in methanol in a sealed vial under nitrogen at 100°C for 45 minutes. Resulting FA methyl esters were extracted with hexane containing 0.05% butylated hydroxytoluene and prepared for GC by sealing the hexane extracts under nitrogen. FA methyl esters were separated and quantified by capillary GC (model 6890; Agilent Technologies) equipped with a 30-m capillary column (DB-88MS; Agilent Technologies) and a flame-ionization detector.

HPLC for Retinoids

Two 50-μL aliquots were taken of samples of BrM-LLP and plasma lipoproteins and handled under safelight conditions. The first, assayed for unesterified retinol, was mixed with 0.6 mL water and 1.5 mL ethanol and then extracted twice with a double volume of hexane. The second aliquot, assayed for unesterified retinol plus RE, was treated with 1.5 mL 5% potassium hydroxide in ethanol for 15 minutes at 65°C to permit RE hydrolysis and extracted as just described. The difference between unesterified retinol and total retinol accounted for the retinol released by hydrolysis from RE. Extracts were dried under nitrogen and resolubilized in 200 μL of HPLC mobile phase. Reversed-phase separation was performed using a separation

module (model 2695; Waters, Milford, MA) with a photograph diode array detector (model 2996; Waters) and a silica-based column (Supelcosil Suplex; pKB100 column; 250 × 4.6 mm, 5 μM; Sigma-Aldrich) equipped with a C18 guard column (Symmetry; Waters). The isocratic mobile phase consisted of 79% acetonitrile, 16% 0.25 M ammonium acetate, 3% glacial acetic acid, and 2% methanol. The flow rate was 0.7 mL/min. Chromatograms were extracted at 325 nm. Retinol peaks were identified by matching spectra and elution times to those of retinol standards. Under-the-curve areas of retinol peaks were converted to molar content using calibration coefficients obtained by separating retinol standards of known concentrations under the same conditions. Plasma lipoprotein RE contents (Supplementary Table S1, column 12, http://www.iovs.org/cgi/content/full/50/2/870/DC1) were comparable to values reported for postprandial normolipemic subjects[19] (i.e., high in CM, moderate in VLDL, and low to trace in LDL).

Cell Culture, Secretion, and Immunoprecipitation

RPE-J cells (from American Type Culture Collection, Manassas, VA) were used for secretion after two passages. The cells were cultured in T-75 flasks at 33°C and 5% CO_2 for 6 days in DMEM and 4% fetal calf serum. Although the long-chain FA oleate is typically used to elicit apoB secretion from hepatoma cells,[20] preliminary experiments indicated that RPE-J responded better to palmitate. Serum-free DMEM containing 0.2 μM palmitate bound to 1.5% FA free-BSA was warmed to 33°C and added into flasks. To detect newly synthesized apoB, 10 mL serum- and methionine-free DMEM containing 100 μL [^{35}S]-methionine (10.5 μCi/μL) were also added. After 4 hours, medium was replaced with serum-free DMEM and incubated for another 4 hours. The medium was centrifuged at 5000 rpm for 5 minutes to remove cellular debris, and the supernatant was subjected to density gradient ultracentrifugation before TLC, electron microscopy,[13] or immunoprecipitation, as follows. The cells were washed with cold PBS, and protein was extracted. [^{35}S]-methionine-labeled cell extract and either whole or fractionated conditioned medium was immunoprecipitated with polyclonal rabbit anti-rat apoB-100 (5 mg/mL; gift of Janet Sparks, University of Rochester, NY) bound to protein-G Sepharose, eluted, resolved with a 5% polyacrylamide gel containing SDS, enhanced by agitation in fluorographic reagent (Amplify; GE Healthcare, Piscataway NJ), and exposed to film. The gel, which also contained LDL and molecular weight markers, was stained with Coomassie blue and superimposed on the film, to permit band verification.

Yield of Particles Isolated from BrM/Choroid: Determination of Nanomoles per Eye

EC is localized almost exclusively to BrM (Rudolf M, et al. *IOVS* 2007;48:ARVO E-Abstract 2184). EC was therefore more suitable for yield calculations than either protein or other lipids such as UC that are present not only in BrM but are also abundant throughout the choroid. We determined EC content in BrM-LLP and BrM remainders of each donor eye pair using an enzymatic assay.[13] Yield, calculated for each donor as (nmol/mL EC in BrM-LLP)/(nmol/mL EC in BrM-LLP + nmol/mL EC in BrM remainder), varied from 32% to 73% (median, 60%), with no obvious relation to age or maculopathy status. This value was used in calculating nanomoles per eye for each lipid class except SPM, which was independently assayed by TLC and quantified. SPM yield ranged from 49% to 66% (median, 53%), comparable to yields for EC and for lipoprotein particles similarly released from atherosclerotic intima.[17]

Determination of Nanomoles per Square Millimeter

Total yield-corrected BrM-LLP-derived lipid was expressed per square millimeter of BrM/choroid, so that we could compare our results directly with previous studies.[16] We determined the area of flattened BrM/choroids using digital planimetry (IPLab; BioVision Technologies). This area was 843 ± 130 mm^2 for individual eyes. Lipid quantities were converted to

micrograms per square millimeters using the formula weight of a representative compound for each lipid class (e.g., cholesteryl oleate for EC, triolein for TG).

Additional Methods

Methods for Western blot analysis, enzymatic cholesterol assay, and negative stain electron microscopy were described previously.[13]

Results

We preliminarily assayed BrM/choroid lipids with TLC, as done in the early study, concluding that this tissue contained more TG than EC,[16] and we found much less TG than EC (not shown). Then, by lipid profiling of this tissue, we confirmed EC's abundance (1394 nanomoles/g, wet weight, in a 37-year-old donor and 4119 to 5542 nanomoles/g in 3 donors ≥ 74 years). EC mass exceeded that of TG by 4.6- to 13.9-fold among individual donors. Such compositional analyses of BrM/choroid unavoidably combine neutral lipids of BrM with membrane-associated UC and PL within choroidal cells and plasma lipoproteins retained in vessels. Therefore, we next isolated and characterized BrM-LLP in seven donors. The top fractions of BrM homogenates contained numerous spherical electron-lucent particles (Fig. 1C),[13] whereas the bottom fractions contained amorphous, heterogeneous material not clearly identifiable as particles (not shown). Particle diameters varied from 11.3 to 211.6 nm in a single-mode, with a positively skewed distribution with a median of 66.6 nm (Fig. 1D), similar to VLDL, and in good agreement with LLP diameters measured in situ.[21] We previously showed that this fraction contains apoA-I and apoB.[13] Here, we detected apoE, a ubiquitous druse component, [9,11,22] by Western blot analysis in both fractions of BrM homogenates (Fig. 1E), indicating that in addition to high-density forms, apoE may also be present on the large LLP.

The BrM-LLP lipid profile, corrected for yield, is summarized in Table 2 (columns 1 to 10), and the plasma lipoprotein profile is shown in Supplementary Table S1, http://www.iovs.org/cgi/content/full/50/2/870/DC1. The BrM-LLP fraction contained 791.8 ± 376.8 nanomoles total lipid per eye, and each square millimeter of BrM contained 0.44 ± 0.16 nanomoles of LLP-derived lipids. Lipid classes, in order of descending abundance, were EC, UC, PC, PE, FA, PS, TG, CL, DAG, and LyPC. EC constituted 32.4% ± 7.9% of the total. EC mass, the most variable lipid, varied sevenfold among donors (Table 2), without obvious explanation, but conforming to histochemical descriptions.[7] BrM-LLP differed notably from plasma lipoproteins in several ways (Table 3). The mean EC/TG ratio was 11.3 ± 6.7, compared to 0.11, 0.13, and 8.5 for CM, VLDL, and LDL, respectively. Thus, BrM-LLP were not TG-rich like CM or VLDL, and their EC/TG ratio was high, similar to LDL. BrM-LLP PL were also distinct, with the PC/PE ratio much lower than that for plasma lipoproteins (1.29 ± 0.19 vs. 6.0 to 14.9; Table 3). Because lipid profiling did not include SPM, which is more closely associated with UC than other PL in plasma membranes, [23] we determined the SPM content independently (Table 2, column 11). We found 79.5 ± 11.1 nmol/eye SPM, and the ratio of SPM to PC measured on the same TLC plates was 0.70 ± 0.13, much higher than the 0.28 to 0.37 ratio in plasma lipoproteins (Table 3). Finally, CL and PS were detected in BrM-LLP but not in plasma lipoproteins (Table 2 versus Supplementary Table S1, http://www.iovs.org/cgi/content/full/50/2/870/DC1).

Of the plasma apoB lipoproteins, only the neutral lipid core of (small-diameter) LDL is as enriched in EC relative to TG as are BrM-LLP. LDL attains this status through the action of lecithin cholesterol acyl transferase, which acts on PC and UC in circulating HDL to form LyPC and EC products that are subsequently transferred to LDL by cholesteryl ester transfer protein. It is important to determine whether high EC content was possible for newly synthesized lipoproteins as well as those released from BrM, where they may have been subjected to similar metabolic remodeling in the extracellular compartment. We therefore

examined the secretory output of RPE-J, a heat-transformed, rat-derived RPE cell line[24] that reportedly secretes protein robustly in culture.[25] First, we verified that lipoprotein assembly and secretion was possible for these cells by seeking evidence of apoB and MTP expression and of particle formation (Fig. 2). Western blot analysis revealed the MTP large subunit at the predicted 97-kDa locations in liver and RPE-J (Fig. 2A). When the RPE-J cells were provided with palmitate and [^{35}S]-methionine, newly synthesized apoB-100, and a low-molecular-weight band were secreted into the whole medium (Fig. 2B) and its top fraction (Fig. 2C). This fraction also contained numerous spherical particles with a mean diameter of 56 nm (Figs. 2D, 2E). We then used TLC to determine the lipid composition of RPE-J-conditioned medium and cells (Fig. 2F). In the particle-containing the top fraction, the EC/TG ratio was 5.6. The cells were similarly EC-rich. For BrM-LLP on the same TLC plate (Fig. 2F), the EC/TG ratio was 8.9.

In lipoprotein-secreting cells, the pathways contributing to the neutral lipid core reflect different input lipids from those contributing to the PL-rich surface.[26,27] To provide insight into potential sources of BrM-LLP lipids, we examined the distribution of FA in neutral lipids and PL of BrM-LLP and plasma lipoproteins (FA with mol% >1% in Fig. 3, all FA in Supplementary Table S2, http://www.iovs.org/cgi/content/full/50/2/870/DC1; see Fig. 3 caption for FA nomenclature). Of FA esterified to cholesterol (Fig. 3A), linoleate (18:2n6) was the most abundant (41.7 ± 4.7 mol%), followed by oleate (18:1n9; 18.4 ± 1.3 mol%), palmitate (16:0; 15.6 ± 1.6 mol%), arachidonate (20:4n6; 7.8 ± 1.3 mol%), and myristate (14:0; 5.1 ± 2.5 mol%). Relative to non-esterified FA and FA in TG (Figs. 3B, 3C), FA in EC included less 16:0, 18:0, and 18:1. Of the PC FA (Fig. 3D), palmitate (16:0) was the most abundant (35.6 ± 2.7 mol%), followed by oleate (18:1n9; 17.8 ± 1.7 mol%), stearate (18:0; 13.2 ± 1.1 mol%), linoleate (18:2n6; 12.6 ± 1.9 mol%), and arachidonate (20:4n6; 9.7 ± 0.79 mol%). PE and PS (Fig. 3E, 3F) differed from PC by having much less palmitate (9%– 12%) and more DHA (but still <2 mol%). Within each lipid class, BrM-LLP FA were overall remarkably similar to plasma lipoproteins, with the principal exception of lower linoleate (18:2n6) among nonesterified FA, TG, PC, and PE. Notably scarce in any BrM-LLP lipid class was the photoreceptor-abundant FA DHA (0.5 ± 0.1 mol% in EC, 1.0 ± 0.4 mol% in PC).

We previously speculated that a presumptively TG-rich BrM-LLP would be an excellent mechanism whereby the RPE could dispose of FA generated from PL in membranes of ingested photoreceptor outer segments (OS).[12] The paucity of TG and DHA in BrM-LLP prompted us to consider other hypotheses about major functions of this particle. Because dietary CMs transport the lipophilic vitamins A, E, and K, and mammalian RPE has been recently postulated to efflux retinoids,[28] we asked whether BrM-LLP contain RE. Figures 4A and 4B show that no free retinol was detectable in the top fraction, but after hydrolysis, released retinol was readily detectable at widely ranging picomolar levels (24–768 pmol/mL) in six of seven tested donor eye pairs. Neither free nor released retinol was detected in the bottom fraction (not shown). The median RE content (yield-corrected) in BrM-LLP of individual eyes was 52 picomoles (Table 2, column 12).

Discussion

The universal and sizeable age-related deposition of neutral lipid in BrM is an enigmatic antecedent of cholesterol-containing drusen and BlinD in ARM eyes. Information from human eyes presented herein will help constrain and inform emerging mouse models, generated by manipulating apolipoprotein pathways, that exhibit different degrees of BrM lipid deposition.[29–33] Our principal findings, obtained with comprehensive lipid assays, are that BrM-LLP are EC-rich, not TG-rich, as predicted by their size. Secretion of apoB and comparably cholesterol-rich particles can be elicited from an FA-supplemented RPE cell line in vitro, BrM-LLP FA composition resembles plasma LDL more than it does photoreceptor OS, and BrM-

LLP contain RE. Obvious differences were not detected between ARM and non-ARM eyes, but due to the choice of lipids analyzed and the small sample, it is premature to conclude that LLP composition in ARM and normal eyes are identical. Herein, we relate our data to BrM-LLP source cells, core composition, and input lipids, with implications for ARM pathogenesis and for retinoid biology.

BrM-LLP reside in a tissue bounded on one side by plasma in the choroid and on the other side by RPE, making determining the predominant source a challenge. For example, LDL could infiltrate from plasma into BrM, become modified, and fuse to form larger particles, as it does in intima,[34] although such fusion is rarely observed in BrM.[8] In the present study, we showed that an RPE cell line has an apparently functional mechanism for apoB biosynthesis, assembly, and secretion. We chose for these experiments the rat-derived cell line RPE-J, although cognizant that key facets of lipoprotein metabolism differ in rats and humans. In brief, rats carry plasma cholesterol principally in HDL rather than LDL, they lack the cholesterol ester transfer protein, and they synthesize apoB-48 in hepatocytes as well as enterocytes.[35,36] Nevertheless, we were able to demonstrate that RPE-J extracts and medium contained a high-molecular-weight band readily immunoprecipitable by an antibody with documented specificity for rat apoB.[37] We also detected a solitary lower molecular weight band at a location consistent with apoB-48 (unlike human RPE[11,12]). Easily proteolyzed apoB-100 is vulnerable to oxidative degradation in our iron-containing culture medium, but had this process occurred, we may have expected many low-weight bands instead of just one. As no in situ evidence for LLP in the extracellular matrix apical to RPE yet exists, basolateral secretion is the currently most plausible mechanism to account for BrM-LLP. We proceed under this assumption, but acknowledge that many details of an RPE apoB pathway require further elucidation and that a plasma contribution to BrM lipids is not excluded.

From our observations that EC is the dominant neutral lipid in nonhomogenized BrM/choroid and that RPE-J cells produce EC-rich large particles in culture, we infer that the high cholesterol content of BrM-LLP is not attributable to transfer or degradation of TG from originally TG-rich particles. The RPE appears unique among apoB secretors in producing a particle that is EC-rich by direct biosynthesis rather than by postsecretion metabolic remodeling, although we cannot yet exclude a role for secreted enzymes. What controls the EC/TG ratio in a lipoprotein core? The predictable apoB lipoprotein size and composition relationship, wherein circulating particles become EC-rich as they shrink from CM to remnants and from VLDL to LDL, reflects in part conformations imposed by particle surface curvature for lipases and transferases. Less clear is what governs EC/TG in nascent lipoproteins, typically studied in culture to escape these plasma effects. Overexpression in hepatoma cells of mRNA encoding cellular enzymes catalyzing esterification of either glycerol or cholesterol to fatty acyl Co-A (DGAT-1,-2 and ACAT-1,-2, respectively[4]) can modify neutral lipid composition, suggesting that adequate stores of either EC or TG can permit particle maturation.[4] Indeed, overexpression of ACAT-2, expressed by lipoprotein-secreting hepatocytes and enterocytes, can convert cells from secreting strongly TG-rich particles to secreting strongly EC-rich particles.[38] RPE cell lines, initially thought to express only the more widely distributed ACAT1,[12] have been recently shown to express ACAT2[39] as well. The cell type–specific balance in activity between these two esterification mechanisms remains to be determined for RPE.

What is the ultimate source of lipids feeding into BrM-LLP? It has long been expected that the daily ingestion of photoreceptor OS by RPE results in the export of material to BrM.[40] We postulated that a TG-rich apoB lipoprotein would be an excellent mechanism for releasing FA derived from PL in OS membranes. Current and previously published compositional data from BrM, LLP, and OS together provide little evidence for this initially attractive hypothesis. First, OS phagocytosis is not essential for neutral lipid secretion, based on experiments using FA supplementation of RPE cell lines.[12] Second, BrM-LLP are not TG-rich, shown in our study

by LC-GC and TLC and previously by two other techniques.[6,13] Each method has strengths and limitations, but all data agree that the original report[16] of high TG mass in BrM/choroid cannot be replicated. (Our assays of BrM/choroid recovered 5.6- to 7.8-fold more total lipid, depending on assumptions, than reported in Ref. 16) Third, BrM-LLP are highly enriched in both EC,[7] absent from photoreceptors, and UC, sparse in the discs that constitute most OS membranes.[41] Fourth, the FA composition of neither the neutral lipids of the BrM-LLP core nor the PL of its surface resemble OS, particularly regarding the top three components: DHA, stearate, and palmitate.[42] We offer several explanations. First, OS lipids may be thoroughly catabolized by RPE before resynthesis as particle components. Second, DHA is efficiently recycled back to the retina,[43] leaving little for export. Third, OS-derived lipids may be present in a form (e.g., oxidized[44]) not recognizable by our assays. Fourth, some lipid classes may be selectively and extensively hydrolyzed in the extracellular compartment after secretion (e.g., by choroid-resident[45] or RPE-secreted lipases), now a less likely option based on our analysis of whole choroid and RPE-J conditioned medium. Fifth, another input may dominate BrM-LLP, which compositionally resemble LDL more than they do OS, despite low linoleate levels. LDL taken up at RPE LDL receptors[46,47] can modify lysosomal acid lipase activity and can partition rapidly, within hours, into membranes of the neurosensory retina.[48] In this way, retina is unlike brain, which eschews plasma lipoprotein cholesterol and relies almost exclusively on endogenous synthesis.[49] Further, the ARPE-19 cell line can take up xanthophylls destined for macular pigment, normally transported in plasma on lipoproteins, via a basally expressed scavenger receptor.[50] Rather than disposing of OS, then, perhaps BrM-LLP dispose of the residual components of plasma lipoproteins after extracting specific nutrients.

The EC-enrichment of BrM-LLP has implications for ARM pathogenesis with regard to transport properties and lesion formation. In vivo BrM-LLP preferentially accumulate in the middle and inner layers of BrM (closer to the RPE), occupying one eighth of the tissue volume at those sites in eyes aged >60 years.[8,21] In the Lipid Wall, located closest to the RPE in the same horizontal plane as BlinD, tightly packed layers of BrM-LLP fill more than one third of tissue volume.[7] The barrier hypothesis posits that this age-related accumulation of neutral lipids blocks translocation of nutrients to the RPE and photoreceptors as well as the outward flow of fluid and metabolites, thereby causing deleterious cellular stress.[5,51] EC is the most hydrophobic lipid in mammalian physiology,[52] indicating that aged BrM, particularly in eyes with a Lipid Wall,[7,53] should indeed present a formidable barrier. Our data may facilitate the construction of and informed experimentation with in vitro model systems to study transport across natural and artificial matrices, perhaps using readily available LDL as an acceptable surrogate because of its high EC content.[54] Further, survival of healthy RPE transplanted to aged BrM[55] may be improved by EC-solubilizing treatments. With regard to lesion formation, cholesterol crystals, the hallmark of a mature atherosclerotic plaque, have never been described in BrM or drusen. A previous speculation[56] that high TG levels[16] could maintain EC solubility and forestall crystal development is rendered untenable by the current data. Of relevance is our detecting UC-avid SPM in higher concentrations (SPM/PC = 0.7) than reported for plasma lipoproteins (SPM/PC $\leq$ 0.3) but in lower concentrations than in insoluble plaque (SPM/PC = 1.6).[57] That BrM-LLP contain abundant EC supports the interpretation that BlinD/drusen contain ultrastructurally visible pooled EC, like that in atherosclerotic intima.[56,58,59]

Of particular interest is the finding that BrM-LLP contain RE, with high between-individual variability (in mol%) perhaps due to uncontrolled exposure to light postmortem. Vitamin A derivatives are required for normal phototransduction, and retinol is delivered to RPE for STRA6-mediated uptake by serum retinol binding protein (SRBP).[60] A recent whole-body radiolabeled tracer study in wild-type mice and mice deficient in RPE65, an essential retinoid isomerohydrolase, provided evidence that RPE also exhibits a robust efflux of retinoids,[29] without specifying the mechanism by which it occurs. Of apoB-producing organs, only intestine incorporates locally esterified retinol into a lipoprotein, and CM remnants deliver

significant retinoid levels to nonhepatic tissues. The liver, in contrast, releases retinol stored in stellate cells to SRBP.[61] Because the RPE expresses lecithin retinol acyl transferase, which catalyzes retinol esterification,[62] it is a plausible source of BrM-LLP RE. It would be remarkable if nature borrowed a CM-like mechanism as a vehicle for retinoid removal in the eye.

Supplementary Material

Refer to Web version on PubMed Central for supplementary material.

Acknowledgments

The authors thank the Alabama Eye Bank for timely retrieval of donor eyes, the staff of Lipomics (Tracy Shafizadeh, PhD, Scientific Alliance Manager) for lipid profiling, and Janet Sparks (University of Rochester) for providing antibody to rat apoB.

Supported by National Institutes of Health (NIH) Grant EY06109 (CAC); the EyeSight Foundation of Alabama (CAC); the Macula Vision Research Foundation (CAC); Deutsche Forschungsgemeinschaft (MR); NIH grant AA12153 (NYK); and Research to Prevent Blindness, Inc. (CAC).

References

1. Council, NAE. Vision Research—A National Plan: 1999–2003, Executive Summary. Washington, DC: National Eye Institute, National Institutes of Health; 1999.
2. Sarks SH. Ageing and degeneration in the macular region: a clinicopathological study. Br J Ophthalmol 1976;60:324–341. [PubMed: 952802]
3. Edwards AO, Malek G. Molecular genetics of AMD and current animal models. Angiogenesis 2007;10:119–132. [PubMed: 17372852]
4. Liang JJ, Oelkers P, Guo C, et al. Overexpression of human diacylglycerol acyltransferase 1, acyl-CoA:cholesterol acyltransferase 1 or acyl-CoA:cholesterol acyltransferase 2 stimulates secretion of apolipoprotein B-containing lipoproteins in McA-RH7777 cells. J Biol Chem 2004;279(43):44938–44944. [PubMed: 15308631]
5. Pauleikhoff D, Harper CA, Marshall J, Bird AC. Aging changes in Bruch's membrane: a histochemical and morphological study. Ophthalmology 1990;97:171–178. [PubMed: 1691475]
6. Haimovici R, Gantz DL, Rumelt S, Freddo TF, Small DM. The lipid composition of drusen, Bruch's membrane, and sclera by hot stage polarizing microscopy. Invest Ophthalmol Vis Sci 2001;42:1592–1599. [PubMed: 11381066]
7. Curcio CA, Millican CL, Bailey T, Kruth HS. Accumulation of cholesterol with age in human Bruch's membrane. Invest Ophthalmol Vis Sci 2001;42:265–274. [PubMed: 11133878]
8. Huang J-D, Presley JB, Chimento MF, Curcio CA, Johnson M. Age-related changes in human macular Bruch's membrane as seen by quick-freeze/deep-etch. Exp Eye Res 2007;85:202–218. [PubMed: 17586493]
9. Li C-M, Clark ME, Chimento MF, Curcio CA. Apolipoprotein localization in isolated drusen and retinal apolipoprotein gene expression. Invest Ophthalmol Vis Sci 2006;47:3119–3128. [PubMed: 16799058]
10. Smith EB. The relationship between plasma and tissue lipids in human atherosclerosis. Adv Lipid Res 1974;12:1– 49. [PubMed: 4371518]
11. Malek G, Li C-M, Guidry C, Medeiros NE, Curcio CA. Apolipoprotein B in cholesterol-containing drusen and basal deposits in eyes with age-related maculopathy. Am J Pathol 2003;162:413–425. [PubMed: 12547700]
12. Li C-M, Presley JB, Zhang X, et al. Retina expresses microsomal triglyceride transfer protein: implications for age-related maculopathy. J Lipid Res 2005;46:628–640. [PubMed: 15654125]
13. Li C-M, Chung BH, Presley JB, et al. Lipoprotein-like particles and cholesteryl esters in human Bruch's membrane: initial characterization. Invest Ophthalmol Vis Sci 2005;46:2576–2586. [PubMed: 15980251]

14. Ishida BY, Bailey KR, Duncan KG, et al. Regulated expression of apolipoprotein E by human retinal pigment epithelial cells. J Lipid Res 2004;45:263–271. [PubMed: 14594998]
15. Jonas, A. Lipoprotein structure. In: Vance, DE.; Vance, JE., editors. Biochemistry of Lipids, Lipoproteins and Membranes. Amsterdam: Elsevier; 2002. p. 483-504.
16. Holz FG, Sheraidah G, Pauleikhoff D, Bird AC. Analysis of lipid deposits extracted from human macular and peripheral Bruch's membrane. Arch Ophthalmol 1994;112:402–406. [PubMed: 8129668]
17. Chung BH, Tallis G, Yalamoori V, Anantharamaiah GM, Segrest JP. Liposome-like particles isolated from human atherosclerotic plaques are structurally and compositionally similar to surface remnants of triglyceride-rich lipoproteins. Arterioscler Thromb 1994;14:622–635. [PubMed: 8148360]
18. Folch P, Lees M, Sloane-Stanley GH. A simple method for the purification of total lipids from animal tissues. J Biol Chem 1957;226:497–509. [PubMed: 13428781]
19. Krasinski SD, Cohn JS, Russell RM, Schaefer EJ. Postprandial plasma vitamin A metabolism in humans: a reassessment of the use of plasma retinyl esters as markers for intestinally derived chylomicrons and their remnants. Metabolism 1990;39:357–365. [PubMed: 2325560]
20. Dixon JL, Furukawa S, Ginsberg HN. Oleate stimulates secretion of apolipoprotein B-containing lipoproteins from Hep G2 cells by inhibiting early intracellular degradation of apolipoprotein B. J Biol Chem 1991;266:5080–5086. [PubMed: 1848237]
21. Huang J-D, Curcio CA, Johnson M. Morphometric analysis of lipoprotein- like particle accumulation in aging human macular Bruch's membrane. Invest Ophthalmol Vis Sci 2008;49:2721– 2727. [PubMed: 18296655]
22. Anderson DH, Ozaki S, Nealon M, et al. Local cellular sources of apolipoprotein E in the human retina and retinal pigmented epithelium: implications for the process of drusen formation. Am J Ophthalmol 2001;131:767–781. [PubMed: 11384575]
23. Demel RA, Jansen JW, van Dijck PW, van Deenen LL. The preferential interaction of cholesterol with different classes of phospholipids. Biochim Biophys Acta 1977;465:1–10. [PubMed: 836830]
24. Nabi IR, Mathews AP, Cohen-Gould L, Gundersen D, Rodriguez-Boulan E. Immortalization of polarized rat retinal pigment epithelium. J Cell Sci 1993;104:37–49. [PubMed: 8383696]
25. Marmorstein LY, Munier FL, Arsenijevic Y, et al. Aberrant accumulation of EFEMP1 underlies drusen formation in Malattia Leventinese and age-related macular degeneration. Proc Natl Acad Sci U S A 2002;99:13067–13072. [PubMed: 12242346]
26. Vance DE. Role of phosphatidylcholine biosynthesis in the regulation of lipoprotein homeostasis. Curr Opin Lipidol 2008;19:229–234. [PubMed: 18460912]
27. Gibbons GF, Wiggins D, Brown AM, Hebbachi AM. Synthesis and function of hepatic very-low-density lipoprotein. Biochem Soc Trans 2004;32:59–64. [PubMed: 14748713]
28. Qtaishat NM, Redmond TM, Pepperberg DR. Acute radiolabeling of retinoids in eye tissues of normal and rpe65-deficient mice. Invest Ophthalmol Vis Sci 2003;44:1435–1446. [PubMed: 12657577]
29. Kliffen M, Lutgens E, Daemen MJAP, de Muinck ED, Mooy CM, de Jong PTVM. The APO*E3-Leiden mouse as an animal model for basal laminar deposit. Br J Ophthalmol 2000;84:1415–1419. [PubMed: 11090485]
30. Dithmar S, Curcio C, Le N-A, Brown S, Grossniklaus H. Ultrastructural changes in Bruch's membrane of apolipoprotein E-deficient mice. Invest Ophthalmol Vis Sci 2000;41:2035–2042. [PubMed: 10892840]
31. Malek G, Johnson LV, Mace BE, et al. Apolipoprotein E allele-dependent pathogenesis: a model for age-related retinal degeneration. Proc Natl Acad Sci U S A 2005;102:11900–11905. [PubMed: 16079201]
32. Rudolf M, Winkler B, Aherrahou Z, Doehring LC, Kaczmarek P, Schmidt-Erfurth U. Increased expression of vascular endothelial growth factor associated with accumulation of lipids in Bruch's membrane of LDL receptor knockout mice. Br J Ophthalmol 2005;89:1627–1630. [PubMed: 16299144]
33. Bretillon L, Acar N, Seeliger MW, et al. ApoB100, LDLR−/− mice exhibit reduced electroretinographic response and cholesteryl esters deposits in the retina. Invest Ophthalmol Vis Sci 2008;49:1307–1314. [PubMed: 18385042]

34. Kruth HS. The fate of lipoprotein cholesterol entering the arterial wall. Curr Opin Lipidol 1997;8:246–252. [PubMed: 9335947]
35. Zak Z, Lagrost L, Gautier T, et al. Expression of simian CETP in normolipidemic Fisher rats has a profound effect on large sized apoE-containing HDL. J Lipid Res 2002;43:2164–2171. [PubMed: 12454279]
36. Sparks CE, Hnatiuk O, Marsh JB. Hepatic and intestinal contribution of two forms of apolipoprotein B to plasma lipoprotein fractions in the rat. Can J Biochem 1981;59:693–699. [PubMed: 7296351]
37. Sparks JD, Zolfaghari R, Sparks CE, Smith HC, Fisher EA. Impaired hepatic apolipoprotein B and E translation in streptozotocin diabetic rats. J Clin Invest 1992;89:1418–1430. [PubMed: 1533230]
38. Temel RE, Hou L, Rudel LL, Shelness GS. ACAT2 stimulates cholesteryl ester secretion in apoB-containing lipoproteins. J Lipid Res 2007;48:1618–1627. [PubMed: 17438337]
39. Yamada Y, Tian J, Yang Y, et al. Oxidized low density lipoproteins induce a pathologic response by retinal pigmented epithelial cells. J Neurochem 2008;105:1187–1197. [PubMed: 18182060]
40. Grindle CFJ, Marshall J. Ageing changes in Bruch's membrane and their functional implications. Trans Ophthalmol Soc U K 1978;98:172–175. [PubMed: 285503]
41. Boesze-Battaglia K, Fliesler SJ, Albert AD. Relationship of cholesterol content to spatial distribution and age of disk membranes in retinal rod outer segments. J Biol Chem 1990;265:18867–18870. [PubMed: 2229047]
42. Rapp LM, Maple SS, Choi JH. Lutein and zeaxanthin concentrations in rod outer segment membranes from perifoveal and peripheral human retina. Invest Ophthalmol Vis Sci 2000;41:1200–1209. [PubMed: 10752961]
43. Bazan NG, Gordon WC, Rodriguez de Turco EB. Docosahexaenoic acid uptake and metabolism in photoreceptors: retinal conservation by an efficient retinal pigment epithelial cell-mediated recycling process. Adv Exp Med Biol 1992;318:295–306. [PubMed: 1386177]
44. Suzuki M, Kamei M, Itabe H, et al. Oxidized phospholipids in the macula increase with age and in eyes with age-related macular degeneration. Mol Vis 2007;13:772–778. [PubMed: 17563727]
45. Casaroli-Marano RP, Peinado-Onsurbe J, Reina M, Staels B, Auwerx J, Vilaro S. Lipoprotein lipase in highly vascularized structures of the eye. J Lipid Res 1996;37:1037–1044. [PubMed: 8725155]
46. Elner VM. Retinal pigment epithelial acid lipase activity and lipoprotein receptors: effects of dietary omega-3 fatty acids. Trans Am Ophthalmol Soc 2002;100:301–338. [PubMed: 12545699]
47. Gordiyenko N, Campos M, Lee JW, Fariss RN, Sztein J, Rodriguez IR. RPE cells internalize low-density lipoprotein (LDL) and oxidized LDL (oxLDL) in large quantities in vitro and in vivo. Invest Ophthalmol Vis Sci 2004;45:2822–2829. [PubMed: 15277509]
48. Tserentsoodol N, Gordiyenko NV, Pascual I, Lee JW, Fliesler SJ, Rodriguez IR. Intraretinal lipid transport is dependent on high density lipoprotein-like particles and class B scavenger receptors. Mol Vis 2006;12:1319–1333. [PubMed: 17110915]
49. Björkhem I, Meaney S. Brain cholesterol: long secret life behind a barrier. Arterioscler Thromb Vasc Biol 2004;5:5.
50. During A, Doraiswamy S, Harrison EH. Xanthophylls are preferentially taken up compared to beta -carotene by retinal cells via a scavenger receptor BI-dependent mechanism. J Lipid Res 2008;49(8): 1715–1724. [PubMed: 18424859]
51. Bird AC, Marshall J. Retinal pigment epithelial detachments in the elderly. Trans Ophthalmol Soc U K 1986;105:674–682. [PubMed: 3310342]
52. Park SW, Addis PB. Capillary column gas-liquid chromatographic resolution of oxidized cholesterol derivatives. Anal Biochem 1985;149:275–283. [PubMed: 4073482]
53. Ruberti JW, Curcio CA, Millican CL, Menco BP, Huang JD, Johnson M. Quick-freeze/deep-etch visualization of age-related lipid accumulation in Bruch's membrane. Invest Ophthalmol Vis Sci 2003;44:1753–1759. [PubMed: 12657618]
54. McCarty WJ, Chimento MF, Curcio CA, Johnson M. Effects of particulates and lipids on the hydraulic conductivity of Matrigel. J Appl Physiol 2008;105(2):621– 628. [PubMed: 18535138]
55. Gullapalli VK, Sugino IK, Zarbin MA. Culture-induced increase in alpha integrin subunit expression in retinal pigment epithelium is important for improved resurfacing of aged human Bruch's membrane. Exp Eye Res 2008;86:189–200. [PubMed: 18062966]

56. Curcio CA, Presley JB, Millican CL, Medeiros NE. Basal deposits and drusen in eyes with age-related maculopathy: evidence for solid lipid particles. Exp Eye Res 2005;80:761–775. [PubMed: 15939032]
57. Chung BH, Mishra V, Franklin F, Liang P, Doran S, Curcio CA. Phosphatidylcholine-rich acceptors, but not native HDL or its apolipoproteins, mobilize cholesterol from cholesterol-rich insoluble components of human atherosclerotic plaques. Biochem Biophys Acta 2005;1733:76–89. [PubMed: 15749058]
58. Li C-M, Clark M, Rudolf M, Curcio CA. Distribution and composition of esterified and unesterified cholesterol in extra-macular drusen. Exp Eye Res 2007;85:192–201. [PubMed: 17553492]
59. Guyton JR, Klemp KF. The lipid-rich core region of human atherosclerotic fibrous plaques: prevalence of small lipid droplets and vesicles by electron microscopy. Am J Pathol 1989;134:705–717. [PubMed: 2646938]
60. Kawaguchi R, Yu J, Honda J, et al. A membrane receptor for retinol binding protein mediates cellular uptake of vitamin A. Science 2007;315:820–825. [PubMed: 17255476]
61. Harrison EH. Mechanisms of digestion and absorption of dietary vitamin A. Annu Rev Nutr 2005;25:87–103. [PubMed: 16011460]
62. Saari JC, Bredberg DL. Lecithin:retinol acyltransferase in retinal pigment epithelial microsomes. J Biol Chem 1989;264:8636– 8640. [PubMed: 2722792]

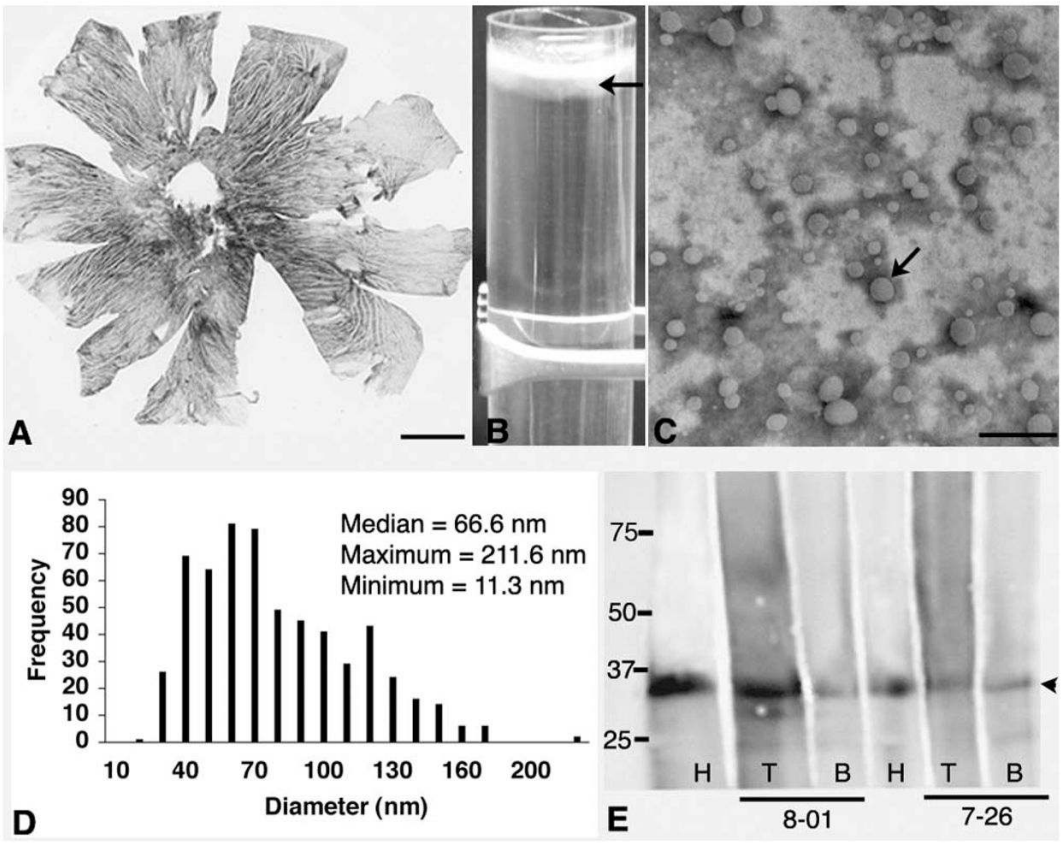

Figure 1.

Preparation of BrM-LLP. (**A**) Flatmounted choroid of human eye. Pigmented stroma is apparent between the clear lumens of large vessels. BrM is the top 2- to 4-μm-thick layer of the choroid. (**B**) Tube contains a cloudy top layer ($d \leq 1.21$ g/mL) containing LLP (*arrow*) below a bright white meniscus. (**C**) Negative-stain electron micrograph of the cloudy layer shows scattered solid, electron-lucent particles (*arrow*). (**D**) Frequency histogram of particle diameters pooled from three donors. (**E**) Western blot shows apoE in HDL (H, positive control) and in the top (T) and bottom (B) fractions of a KBr density gradient from donors 8-01 and 7-26. *Left*: molecular weight standards. *Arrowhead*: ApoE, at 35 kDa. Scale bar: (**A**) 5 mm; (**C**) 500 nm.

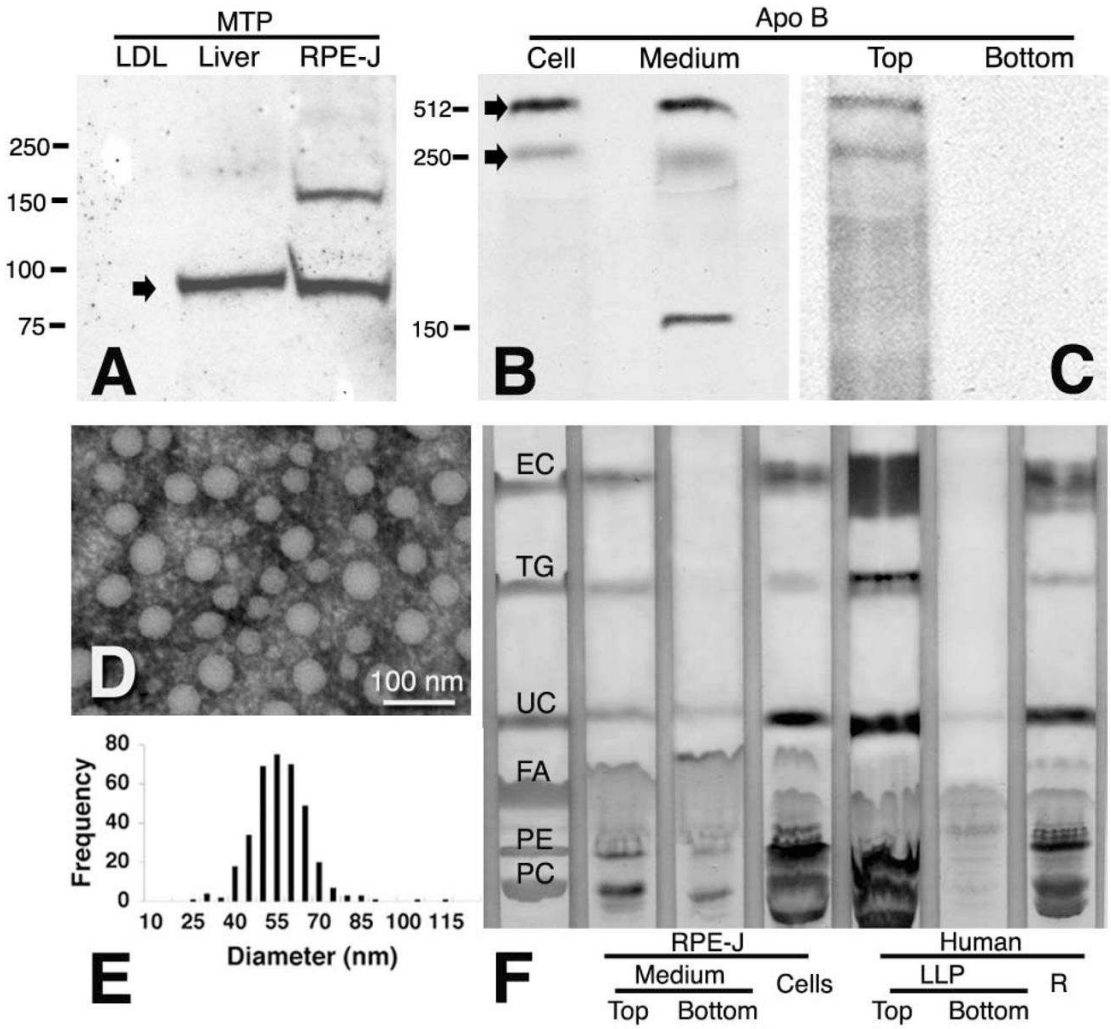

Figure 2.

RPE-J cells synthesize and secrete apoB and EC-rich particles. (**A**) Western blot of MTP in RPE-J cells and rat liver. Human LDL was used as a negative control, because its only protein is apoB. RPE-J cellular protein (100 μg), rat liver protein (10 μg), and LDL (1 μg, sufficient for apoB detection in test blots) were loaded. MTP was found at the predicted 97-kDa location (*arrow*). (**B**, **C**) Immunoprecipitation of [^{35}S]-methionine labeled, newly synthesized apoB in cells and medium of palmitate-supplemented RPE-J cells. *Arrow*: apoB-100 (512 kDa) and a 250-kDa band, possibly apoB-48, in cells and whole medium (**B**), and in the top fraction only of fractionated medium (**C**). (**D**, **E**) A fraction containing RPE-J-secreted particles was examined by electron microscopy after negative staining with phosphotungstic acid (**D**). Frequency histogram of diameters (**E**, n = 489) is from one experiment. (**F**) RPE-J particles and BrM-LLP are both EC-rich. TLC plate shows lanes for standards, top and bottom fractions of medium conditioned by palmitate-supplemented RPE-J cells, RPE-J cells, top and bottom fractions of BrM-LLP from donor 07-29, and BrM/choroid remainder (R) with unreleased particles.

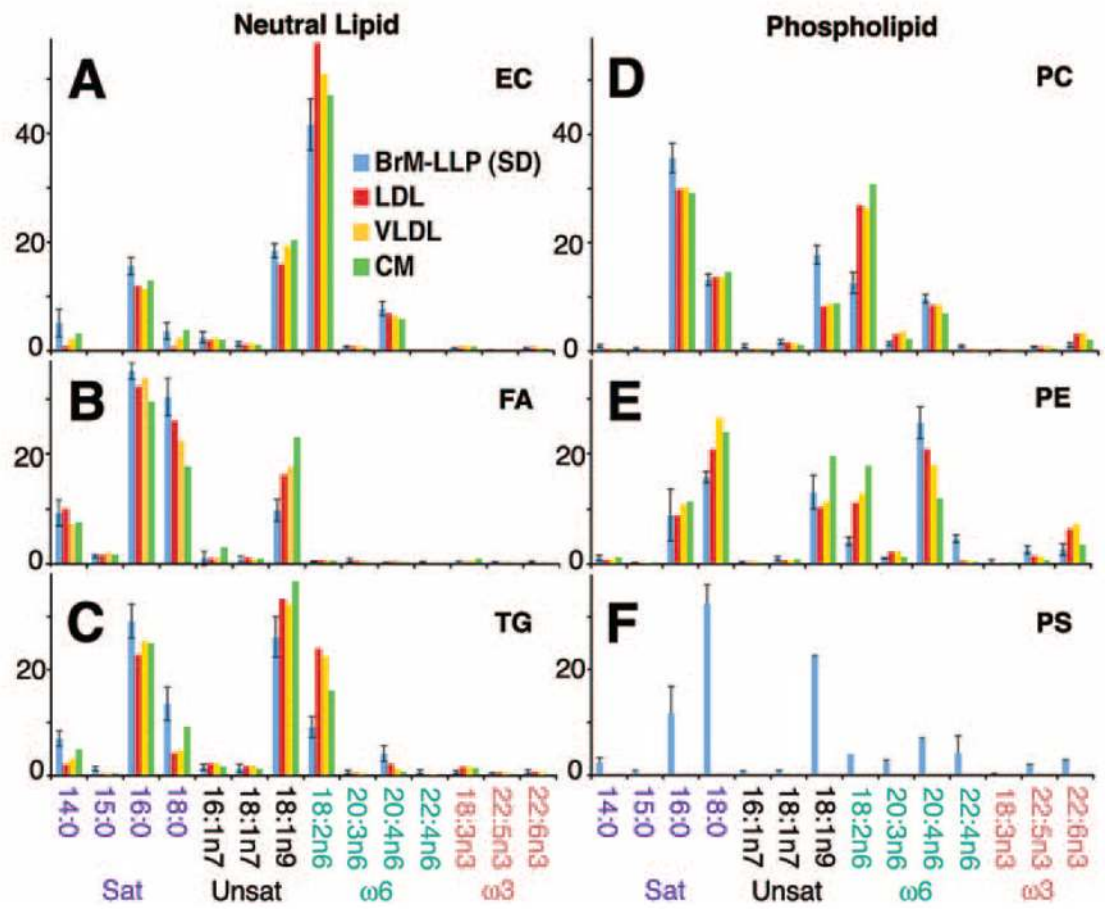

Figure 3.

FA in major lipid classes of BrM-LLP and plasma lipoproteins. Fourteen FA with mol% >1% for any lipoprotein are shown (*y*-axis, mol%). See Supplementary Table S2, http://www.iovs.org/cgi/content/full/50/2/870/DC1, for all FA from all lipid classes. Along the *x*-axis, FA are divided into families as follows: Sat, saturated (no double bonds); Unsat, unsaturated (one or more double bonds, not at the n6 or n3 positions, as produced by the action of Δ9 desaturase and subsequent elongases); ω6 and ω3, omega-6, and omega-3 (double bonds in the n6 and n3 positions, respectively). FA notation: CXX:Yn-Z, where XX is the length of the carbon chain, Y is the number of double bonds along the carbon chain, and Z is the position of the first double bond, counting from the methyl carbon. The enzyme Δ9 desaturase acts on the carbon-9 position, counting from the carboxyl end of the molecule rather than the methyl carbon. Therefore, Δ9 desaturase metabolites named using the *n* nomenclature, as shown in this figure and in Supplementary Table S2, will not all have the first double bond in the 9 position.

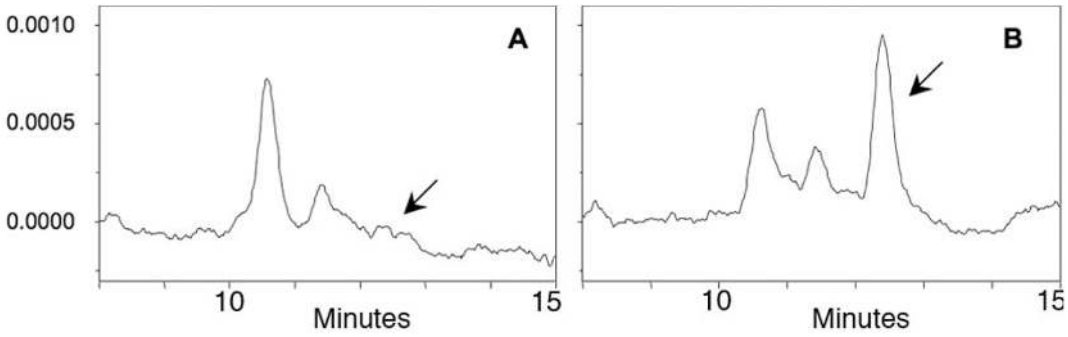

Figure 4.

HPLC detection of RE. BrM-LLP from donor 07-21 were extracted without alkaline hydrolysis to detect free retinol (**A**). An equal aliquot of the same sample was hydrolyzed before extraction to release retinol from esterified forms (**B**). Chromatograms were extracted at 325 nm. *Arrow*: position of retinol. The identity of the large peak is unknown. The *y*-axis represents arbitrary units.

Table 1

Donors and Eyes

ID	Age (y)	Sex	Race*	D to P† (h)	Macular Health‡		Tissue§	Use‖
					Left Eye	Right Eye		
6–08	86	M	Cauc	5:35	n.r.	ARM	BrM/Ch	LC-GC
7–13	74	M	Cauc	6:10	Normal	Normal	BrM/Ch	LC-GC
7–14	78	M	Cauc	6:34	Normal	Normal	BrM/Ch	LC-GC
7–16	72	F	Cauc	8:10	Normal	Normal	LLP, R	LC-GC, HPLC
7–17	37	M	A-A	7:48	Normal	Normal	BrM/Ch	LC-GC
7–18	90	M	Cauc	8:13	Ex-ARM	Early ARM	LLP, R	LC-GC, HPLC, TLC
7–21	85	F	Cauc	21:52	Normal	Normal	LLP, R	LC-GC, HPLC, TLC
7–22	59	M	A-A	9:27	Macular hole	n.r.	LLP, R	LC-GC, HPLC, TLC
7–23	51	M	Cauc	2:55	Normal	Normal	LLP, R	LC-GC, HPLC, TLC
7–24	87	F	Cauc	9:36	Normal	Normal	LLP, R	LC-GC, HPLC, TLC
7–25	86	M	Cauc	12:14	Early ARM	Early ARM	LLP, R	LC-GC, HPLC, TLC
7–26	82	F	Cauc	7:49	Normal	Normal	LLP	TLC, WB
7–27	79	M	Cauc	13:04	Normal	Normal	LLP	EM
7–29	82	M	Cauc	6:22	Early ARM	Early ARM	LLP	EM, TLC
8-01	52	F	Cauc	12:20	Normal	Normal	LLP	EM, WB

*Cauc, Caucasian; A-A, African-American.

†Death to processing time.

‡Assessed by an ophthalmologist; early ARM, drusen and pigmentary changes; Ex-ARM, late exudative ARM; n.r., not recorded; all donors were nondiabetic.

§BrM/Ch, BrM and choroid tissue, shown in Fig. 1A; LLP, particles in $d \leq 1.21$ g/mL fraction; R, remainder (BrM/Ch after LLP removal).

‖LC-GC, lipid profiling by liquid chromatography and gas chromatography; HPLC, high-pressure liquid chromatography; TLC, thin layer chromatography; WB, western blot; EM; negative stain electron microscopy.

Table 2

Lipid Profile of BrM Particles (nmol/eye and mole%, corrected for yield)

	1 EC	2 DG	3 FA	4 TG	5 CL	6 LYPC	7 PC	8 PE	9 PS	10 UC	11 SPM	12 RE
ID												
7–16	193.2	7.9	36.3	18.0	n.a.	n.a.	116.2	90.5	n.a.	159.0	78.0	0.053
7–18	84.7	10.7	29.3	16.0	19.7	14.1	43.9	n.a.	20.5	51.8	n.a.	n.d.
7–21	506.2	13.6	47.1	20.1	19.7	9.0	177.3	112.0	46.9	304.4	82.9	0.040
7–22	210.2	13.7	64.8	30.7	24.9	28.4	116.8	106.0	57.9	215.3	91.9	0.051
7–23	157.8	13.5	45.2	20.4	19.5	9.4	105.2	95.4	49.0	195.2	68.0	0.145
7–24	561.0	15.4	60.0	42.5	41.6	10.3	149.0	103.6	51.6	263.2	90.5	0.403
7–25	180.8	7.3	28.6	17.7	24.6	9.0	59.7	48.0	20.7	100.4	65.7	0.009
Median, nmol/eye	193.2	13.5	45.2	20.1	19.7	9.4	116.2	95.4	46.9	195.2	80.4	0.052
Mean, nmol/eye	270.6	11.7	44.5	23.6	21.4	11.4	109.7	79.4	35.2	184.2	79.5	0.117
SD, nmol/eye	184.8	3.1	14.2	9.6	12.2	8.6	46.6	40.9	21.5	88.5	11.1	0.147
Mean, mole%*	32.4	1.7	6.3	3.3	3.2	1.8	14.2	9.5	4.6	22.9	n.a.	n.a.
SD, mole%*	7.9	0.9	2.1	1.2	2.2	1.7	2.4	4.9	2.5	3.5	n.a.	n.a.

Assays used: columns 1–10, LC-GC; column 11, TLC for polar lipids; column 12, reversed phase HPLC. EC, esterified cholesterol; DG, diglyceride; FA, non-esterified fatty acid; TG, triglyceride; CL, cardiolipin; LYPC, lysophosphatidylcholine; PC, phosphatidylcholine; PE, phosphatidylethanolamine; PS, phosphatidylserine; UC, unesterified cholesterol; SPM, sphingomyelin; RE, retinyl ester; n.a., not available; n.d., not detected.

*Calculated relative to the sum of columns 1–10 for each eye (mean, 791.8 ± 376.8 nmol/eye).

Table 3

BrM-LLP Compared to Plasma LP

	EC/(EC+UC)	EC/TG	PC/PE	SPM/PC
BrM particles (SD)	0.58 (0.085)	11.32(6.676)	1.29(0.190)	0.70(0.13)
CM	0.59	0.11	6.09	0.28*
VLDL	0.45	0.13	8.30	0.28*
LDL	0.69	8.52	14.90	0.37*

* Calculated from Ref. 15.